

Search for the FCNC's $B_s^0 \rightarrow \mu^+\mu^-$ and $B^0 \rightarrow \mu^+\mu^-$ with the LHCb spectrometer

D. Martínez Santos

on behalf of the LHCb Collaboration

European Organization for Nuclear Research (CERN), Geneva, Switzerland

Abstract

A search for the decays $B_s^0 \rightarrow \mu^+\mu^-$ and $B^0 \rightarrow \mu^+\mu^-$ is performed with about 37 pb^{-1} of pp collisions at $\sqrt{s} = 7 \text{ TeV}$ collected by the LHCb experiment at the Large Hadron Collider at CERN. The observed numbers of events are consistent with the background expectations. The resulting upper limits on the branching ratios are $\text{BR}(B_s^0 \rightarrow \mu^+\mu^-) < 5.6 \times 10^{-8}$ and $\text{BR}(B^0 \rightarrow \mu^+\mu^-) < 1.5 \times 10^{-8}$ at 95% confidence level.

1 Introduction

Precision observables at low energy allow access to information at higher energy scales, constraining possible New Physics (NP) scenarios. The branching ratios (BR) $BR(B_{(s)}^0 \rightarrow \mu^+\mu^-)$ have been identified as a very interesting potential constraint on the parameter space of NP models.

The SM prediction for the BR of the decays $B_s^0 \rightarrow \mu^+\mu^-$ and $B^0 \rightarrow \mu^+\mu^-$ have been computed¹ to be $BR(B_s^0 \rightarrow \mu^+\mu^-) = (3.2 \pm 0.2) \times 10^{-9}$ and $BR(B^0 \rightarrow \mu^+\mu^-) = (0.10 \pm 0.01) \times 10^{-9}$.

However NP contributions can significantly modify these values. For example, within Minimal Supersymmetric extensions of the SM (MSSM), the $BR(B_s \rightarrow \mu^+\mu^-)$ has contributions proportional to $\sim \tan^6 \beta^2$, where $\tan \beta$ is the ratio of vacuum expectation values of the two neutral CP-even Higgs fields.

The current published 95% upper limits were obtained using 6.1 fb^{-1} by the D0 collaboration³, $\text{BR}(B_s^0 \rightarrow \mu^+\mu^-) < 5.1 \times 10^{-8}$ and using 2 fb^{-1} by the CDF collaboration⁴, $\text{BR}(B_s^0 \rightarrow \mu^+\mu^-) < 5.8 \times 10^{-8}$ and $\text{BR}(B^0 \rightarrow \mu^+\mu^-) < 1.8 \times 10^{-8}$. The CDF collaboration has also presented preliminary results⁵ with 3.7 fb^{-1} that lower the limits to $\text{BR}(B_s^0 \rightarrow \mu^+\mu^-) < 4.3 \times 10^{-8}$ and $\text{BR}(B^0 \rightarrow \mu^+\mu^-) < 0.76 \times 10^{-8}$.

The LHCb experiment is well suited for such searches due to the high $b\bar{b}$ cross section at LHC, the good invariant mass resolution, vertex resolution, muon identification and trigger efficiency.

The measurements presented in this document use about 37 pb^{-1} of integrated luminosity collected by LHCb between July and October 2010 at $\sqrt{s} = 7 \text{ TeV}$. Assuming the SM branching ratio, about 0.7 (0.08) $B_{(s)}^0 \rightarrow \mu^+\mu^-$ ($B^0 \rightarrow \mu^+\mu^-$) are expected to be reconstructed within LHCb acceptance.

2 The LHCb detector

The LHCb detector⁶ is a single-arm forward spectrometer with an angular coverage from approximately 10 mrad to 300 (250) mrad in the bending (non-bending) plane.

The detector consists of a vertex locator, a warm dipole magnet with a bending power of $\int B dl = 4 \text{ T m}$, a tracking system, two RICH detectors, a calorimeter system and a muon system.

Track momenta are measured with a precision between $\delta p/p = 0.35\%$ at 5 GeV/c and $\delta p/p = 0.5\%$ at 100 GeV/c. The RICH system provides charged hadron identification in a momentum range 2–100 GeV/c. Typically kaon identification efficiencies of over 90% can be attained for a $\pi \rightarrow K$ fake rate below 10%. The calorimeter system consists of a preshower, a scintillating pad detector, an electromagnetic calorimeter and a hadronic calorimeter. It identifies high transverse energy (E_T) hadron, electron and photon candidates and provides

information for the trigger. Five muon stations provide fast information for the trigger and muon identification capability: a muon identification efficiency of $\sim 95\%$ is obtained for a misidentification rate of about 1–2 % for momenta above 10 GeV/c.

LHCb has a two-level flexible and efficient trigger system both for leptonic and purely hadronic B decays. It exploits the finite lifetime and relatively large mass of charm and beauty hadrons to distinguish heavy flavour decays from the dominant light quark processes. The first trigger level (L0) is implemented in hardware and reduces the rate to a maximum of 1 MHz, the read-out rate of the whole detector. The second trigger level (High Level Trigger, HLT) is implemented in software running on an event filter CPU farm. The forward geometry allows the LHCb first level trigger to collect events with one or two muons with p_T values as low as 1.4 GeV/c for single muon and $p_T(\mu_1) > 0.48$ GeV/c and $p_T(\mu_2) > 0.56$ GeV/c for dimuon triggers. During 2010 data taking, the E_T threshold for the hadron trigger varied in the range 2.6 to 3.6 GeV.

The dimuon trigger line requires muon pairs of opposite charge forming a common vertex and an invariant mass $M_{\mu\mu} > 4.7$ GeV/c². A second trigger line, primarily to select $J/\psi \rightarrow \mu\mu$ events, requires $2.97 < M_{\mu\mu} < 3.21$ GeV/c². The remaining region of the dimuon invariant mass is also covered by trigger lines that in addition require the dimuon secondary vertex to be well separated from the primary vertex. Other HLT trigger lines select generic displaced vertices, providing a high efficiency for purely hadronic decays.

3 Analysis Strategy

The analysis for the $B_{(s)}^0 \rightarrow \mu^+\mu^-$ search at LHCb is described in detail in⁷. It is done in two steps: first a set of selection cuts removes the biggest amount of the background while keeping $\sim 60\%$ of the reconstructed signal decays. Then each event is given a probability to be signal or background in a two-dimensional probability space defined by the dimuon invariant mass and a multivariate analysis discriminant likelihood, the *Geometrical Likelihood* (GL)^{10,11}. The compatibility of the observed distribution of events in the GL *vs* invariant mass plane with a given branching ratio hypothesis is computed using the CL_s method⁸.

The number of expected signal events is evaluated by normalizing with channels of known branching ratios: $B^+ \rightarrow J/\psi(\rightarrow \mu^+\mu^-)K^+$, $B_s^0 \rightarrow J/\psi(\rightarrow \mu^+\mu^-)\phi(\rightarrow K^+K^-)$ and $B^0 \rightarrow K^+\pi^-$. This normalization ensures that knowledge of the absolute integrated luminosity and $b\bar{b}$ production cross-section are not needed, and that systematic uncertainties related to the efficiency cancel out in the ratio.

3.1 Event selection

The event selection is designed to reduce the amount of data to analyze, and the real discrimination between signal and background is done by the likelihoods. The selection consists of loose requirements on track separation from the interaction point, decay vertex quality and compatibility of the reconstructed origin of the B meson with the interaction point. The selection cuts were defined in simulation before starting data taking. Events passing the selection are considered $B_{(s)}^0 \rightarrow \mu^+\mu^-$ candidates if their invariant mass lies within 60 MeV/c² of the nominal $B_{(s)}^0$ mass. Assuming the SM branching ratio, There are 343 (342) $B_{(s)}^0 \rightarrow \mu^+\mu^-$ candidates selected from data in the $B_s^0(B^0)$ mass window. A similar selection is applied to the normalization channels, in order to minimize systematic errors in the ratio of efficiencies.

The dominant background after the $B_{(s)}^0 \rightarrow \mu^+\mu^-$ selection is expected to be $b\bar{b} \rightarrow \mu\mu X$ ⁹. This is confirmed by comparing expected yield and the kinematical distributions of the sideband data with a $b\bar{b} \rightarrow \mu\mu X$ MC sample.

The muon misidentification probability as a function of momentum obtained from data using $K_S^0 \rightarrow \pi^+\pi^-$, $\Lambda \rightarrow p\pi^-$ and $\phi \rightarrow K^+K^-$ decays is in good agreement with MC expectations. It is found that the background from misidentified $B_{s,d}^0 \rightarrow h^+h'^-$ is negligible for the amount of data used in this analysis.

3.2 Signal and background likelihoods

After the selection the signal purity is still about 10^{-3} for $B_s^0 \rightarrow \mu^+\mu^-$ and 10^{-4} for $B^0 \rightarrow \mu^+\mu^-$ assuming the SM branching ratios. Further discrimination is achieved through the combination of two independent variables: the multivariate analysis discriminant likelihood, GL, and the invariant mass. The GL combines information related with the topology and kinematics of the event as the $B_{(s)}^0$ lifetime, the minimum impact parameter of the two muons, the distance of closest approach of the two tracks, the $B_{(s)}^0$ impact parameter and p_T and the isolation of the muons with respect to the other tracks of the event. These variables are combined using the method described in ^{10,11}. The expected GL distribution for signal events is flat, while for background events it falls exponentially.

The analysis is performed in two-dimensional bins of invariant mass and GL. The invariant mass in the signal regions (± 60 MeV/ c^2 around the B_s^0 and the B^0 masses) is divided into six bins of equal width, and the GL into four bins of equal width distributed between zero and one. A probability to be signal or background is assigned to events falling in each bin.

The GL variable is defined using MC events but calibrated with data using $B_{s,d}^0 \rightarrow h^+h'^-$ selected as the signal events and triggered independently on the signal in order to avoid the bias introduced by the hadronic trigger lines.

The number of $B_{s,d}^0 \rightarrow h^+h'^-$ events in each GL bin is obtained from a fit to the inclusive mass distribution.

Two methods have been used to estimate the $B_{(s)}^0 \rightarrow \mu^+\mu^-$ mass resolution from data. The first method uses an interpolation between the measured resolutions for $c\bar{c}$ resonances (J/ψ , $\psi(2S)$) and $b\bar{b}$ resonances ($\Upsilon(1S)$, $\Upsilon(2S)$, $\Upsilon(3S)$) decaying into two muons. Interpolating linearly between the five fitted resolutions to $M_{B_s^0}$ an invariant mass resolution of $\sigma = 26.83 \pm 1.0$ MeV/ c^2 was estimated.

The second method that was used to estimate the invariant mass resolution from data is to use the inclusive $B_{s,d}^0 \rightarrow h^+h'^-$ sample. The result of the fit for the mass resolution, $\sigma = 25.8 \pm 2.5$ MeV/ c^2 , is consistent with the value obtained from the interpolation method.

The weighted average of the two methods, $\sigma = 26.7 \pm 0.9$ MeV/ c^2 , is taken as the invariant mass resolution and considered to be the same for B^0 and B_s^0 decays.

The prediction of the number of background events in the signal regions is obtained by fitting with an exponential function the $\mu\mu$ mass sidebands independently in each GL bin. The mass sidebands are defined in the range between $M_{B_{(s)}^0} \pm 600$ (1200) MeV/ c^2 for the lower (upper) two GL bins, excluding the two search windows ($M_{B_{(s)}^0} \pm 60$ MeV/ c^2).

4 Normalization factors

The number of expected signal events is evaluated by normalizing with channels of known branching ratios, $B^+ \rightarrow J/\psi K^+$, $B_s^0 \rightarrow J/\psi \phi$ and $B^0 \rightarrow K^+\pi^-$, as shown in Table 1, first column.

The first two decays have similar trigger and muon identification efficiency to the signal but a different number of particles in the final state, while the third channel has the same two-body topology but cannot be efficiently selected with the muon triggers. The branching ratio of the $B_s^0 \rightarrow J/\psi \phi$ decay is not known precisely ($\sim 25\%$) but has the advantage that the normalization

Table 1: Summary of the factors and their uncertainties needed to calculate the normalization factors ($\alpha_{B_{(s)}^0 \rightarrow \mu^+ \mu^-}$) for the three normalization channels considered. The branching ratios are taken from Refs. ^{12,14} and includes also the $\text{BR}(J/\psi \rightarrow \mu^+ \mu^-)$ and $\text{BR}(\phi \rightarrow K^+ K^-)$. The trigger efficiency and number of $B^0 \rightarrow K^+ \pi^-$ candidates correspond to only TIS events, as described in the text.

	BR ($\times 10^{-5}$)	$\frac{\epsilon_{\text{norm}}^{\text{REC}} \epsilon_{\text{norm}}^{\text{SEL REC}}}{\epsilon_{\text{sig}}^{\text{REC}} \epsilon_{\text{sig}}^{\text{SEL REC}}}$	$\frac{\epsilon_{\text{norm}}^{\text{TRIG SEL}}}{\epsilon_{\text{sig}}^{\text{TRIG SEL}}}$	N_{norm}	$\alpha_{B_{(s)}^0 \rightarrow \mu^+ \mu^-}$ ($\times 10^{-9}$)	$\alpha_{B^0 \rightarrow \mu^+ \mu^-}$ ($\times 10^{-9}$)
$B^+ \rightarrow J/\psi K^+$	5.98 ± 0.22	0.49 ± 0.02	0.96 ± 0.05	$12,366 \pm 403$	8.4 ± 1.3	2.27 ± 0.18
$B_s^0 \rightarrow J/\psi \phi$	3.4 ± 0.9	0.25 ± 0.02	0.96 ± 0.05	760 ± 71	10.5 ± 2.9	2.83 ± 0.86
$B^0 \rightarrow K^+ \pi^-$	1.94 ± 0.06	0.82 ± 0.06	0.072 ± 0.010	578 ± 74	7.3 ± 1.8	1.99 ± 0.40

of $B_{(s)}^0 \rightarrow \mu\mu$ with a B_s^0 decay does not require the knowledge of the ratio of fragmentation fractions, which has an uncertainty of $\sim 13\%$ ¹³.

Using each of these normalization channels, $\text{BR}(B_{(s)}^0 \rightarrow \mu\mu)$ can be calculated as:

$$\begin{aligned}
 \text{BR}(B_{(s)}^0 \rightarrow \mu\mu) &= \text{BR}_{\text{norm}} \times \frac{\epsilon_{\text{norm}}^{\text{REC}} \epsilon_{\text{norm}}^{\text{SEL|REC}} \epsilon_{\text{norm}}^{\text{TRIG|SEL}}}{\epsilon_{\text{sig}}^{\text{REC}} \epsilon_{\text{sig}}^{\text{SEL|REC}} \epsilon_{\text{sig}}^{\text{TRIG|SEL}}} \times \frac{f_{\text{norm}}}{f_{B_{(s)}^0}} \times \frac{N_{B_{(s)}^0 \rightarrow \mu\mu}}{N_{\text{norm}}} \\
 &= \alpha_{B_{(s)}^0 \rightarrow \mu\mu} \times N_{B_{(s)}^0 \rightarrow \mu\mu},
 \end{aligned} \tag{1}$$

where $\alpha_{B_{(s)}^0 \rightarrow \mu\mu}$ denotes the normalization factor, $f_{B_{(s)}^0}$ denotes the probability that a b -quark fragments into a $B_{(s)}^0$ and f_{norm} denotes the probability that a b -quark fragments into the b -hadron relevant for the chosen normalization channel with branching fraction BR_{norm} . The reconstruction efficiency (ϵ^{REC}) includes the acceptance and particle identification, while $\epsilon^{\text{SEL|REC}}$ denotes the selection efficiency on reconstructed events. The trigger efficiency on selected events is denoted by $\epsilon^{\text{TRIG|SEL}}$.

The ratios of reconstruction and selection efficiencies are estimated from the simulation using different levels of smearing on the track parameters and checked with data, while the ratios of trigger efficiencies on selected events are determined from data ¹⁵.

The yields needed to evaluate the normalization factor are shown in Table 1, where the uncertainty is dominated by the differences observed using different models in fitting the invariant mass lineshape.

As can be seen in Table 1, the normalization factors calculated using the three complementary channels give compatible results. The final normalization factor is a weighted average which takes, with the result:

$$\begin{aligned}
 \alpha_{B_{(s)}^0 \rightarrow \mu\mu} &= (8.6 \pm 1.1) \times 10^{-9}, \\
 \alpha_{B^0 \rightarrow \mu\mu} &= (2.24 \pm 0.16) \times 10^{-9}.
 \end{aligned}$$

5 Results

For each of the 24 bins (4 bins in GL and 6 bins in mass) the expected number of background events is computed from the fits to the invariant mass sidebands described in Sect. 3.2. The expected numbers of signal events are computed using the normalization factors from Sect. 4,

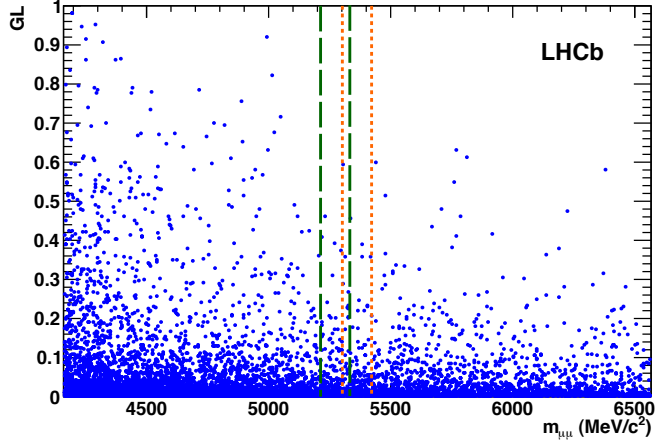


Figure 1: Observed distribution of selected dimuon events in the GL vs invariant mass plane. The orange short-dashed (green long-dashed) lines indicate the ± 60 MeV/c^2 search window around the $B_s^0(B^0)$.

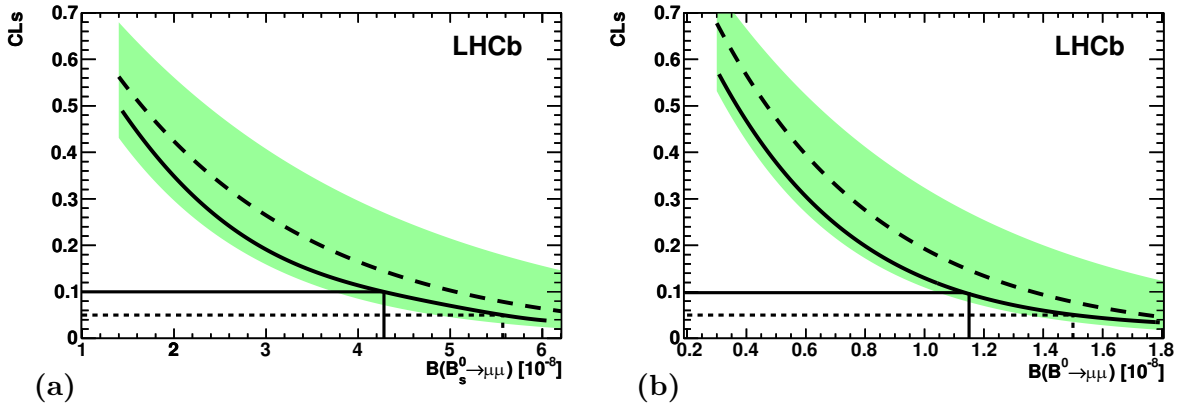


Figure 2: (a) Observed (solid curve) and expected (dashed curve) CL_s values as a function of $\text{BR}(B_s^0 \rightarrow \mu^+\mu^-)$. The green shaded area contains the $\pm 1\sigma$ interval of possible results compatible with the expected value when only background is observed. The 90% (95%) CL observed value is identified by the solid (dashed) line. (b) the same for $\text{BR}(B^0 \rightarrow \mu^+\mu^-)$.

and the signal likelihoods computed in Section 3.2. The distribution of observed events in the GL vs invariant mass plane can be seen in Fig. 1.

The compatibility of the observed distribution of events in the GL vs invariant mass plane with a given branching ratio hypothesis is evaluated using the CL_s method⁸. The observed distribution of CL_s as a function of the assumed branching ratio can be seen in Fig. 2.

The expected distributions of possible values of CL_s assuming the background-only hypothesis are also shown in the same figure as a green shaded area that covers the region of $\pm 1\sigma$ of background compatible observations. The uncertainties in the signal and background likelihoods and normalization factors are used to compute the uncertainties in the background and signal predictions.

The upper limits are computed using the CL_s distributions in Fig. 2 with the results:

$$\begin{aligned} \text{BR}(B_s^0 \rightarrow \mu^+\mu^-) &< 4.3 (5.6) \times 10^{-8} \text{ at } 90\% (95\%) \text{ C.L.}, \\ \text{BR}(B^0 \rightarrow \mu^+\mu^-) &< 1.2 (1.5) \times 10^{-8} \text{ at } 90\% (95\%) \text{ C.L.}, \end{aligned}$$

while the expected values of the limits are $\text{BR}(B_s^0 \rightarrow \mu^+\mu^-) < 5.1 (6.5) \times 10^{-8}$ and $\text{BR}(B^0 \rightarrow \mu^+\mu^-) < 1.4 (1.8) \times 10^{-8}$ at 90% (95%) CL. The limits observed are similar to the best published

limits³ for the decay $B_s^0 \rightarrow \mu^+\mu^-$ and more restrictive for the decay $B^0 \rightarrow \mu^+\mu^-$ ⁴.

References

1. A.J. Buras, “Minimal flavour violation and beyond: Towards a flavour code for short distance dynamics”, arXiv:1012.1447;
E. Gamiz *et al.*, “Neutral B meson mixing in unquenched lattice QCD”, *Phys. Rev.* **D80** (2009) 014503;
A.J. Buras, “Relations between $\Delta M_{s,d}$ and $B_{s,d} \rightarrow \mu^+\mu^-$ in models with Minimal Flavour Violation”, *Phys. Lett.* **B566** (2003) 115.
2. L. J. Hall, R. Rattazzi and U. Sarid, “The top quark mass in supersymmetric SO(10) unification” *Phys. Rev.* **D50** (1994) 7048;
C. Hamzaoui, M. Pospelov and M. Toharia, “Higgs-mediated FCNC in supersymmetric models with large $\tan\beta$ ”, *Phys. Rev.* **D59** (1999) 095005;
K.S. Babu and C.F. Kolda, “Higgs-mediated $B_{s,d} \rightarrow \mu^+\mu^-$ in minimal supersymmetry”, *Phys. Rev. Lett.* **84** (2000) 228.
3. V. Abazov *et al.* [D0 Collaboration], “Search for the rare decay $B_s^0 \rightarrow \mu^+\mu^-$ ”, *Phys. Lett.* **B693** (2010) 539.
4. T. Aaltonen *et al.* [CDF Collaboration], “Search for $B_s^0 \rightarrow \mu^+\mu^-$ and $B_d^0 \rightarrow \mu^+\mu^-$ decays with 2 fb⁻¹ of $p\bar{p}$ Collisions”, *Phys. Rev. Lett.* **100** (2008) 101802.
5. T. Aaltonen *et al.* [CDF Collaboration], “Search for $B_s^0 \rightarrow \mu^+\mu^-$ and $B^0 \rightarrow \mu^+\mu^-$ decays in 3.7 fb⁻¹ of $p\bar{p}$ collisions with CDF II”, CDF Public Note 9892.
6. A.A. Alves *et al.* [LHCb Collaboration], “The LHCb detector at the LHC”, *JINST* **3** (2008) S08005, and references therein.
7. R. Aaji *et al.* [LHCb Collaboration], “Search for the rare decays $B_s^0 \rightarrow \mu^+\mu^-$ and $B^0 \rightarrow \mu^+\mu^-$ ”, *Phys. Lett.* **B699** (2011), 330-340.
8. A.L. Read, “Presentation of search results: the CL_s technique”, *J. Phys.* **G28** (2002) 2693;
T. Junk, “Confidence level computation for combining searches with small statistics”, *Nucl. Instrum. Methods* **A434** (1999) 435.
9. B. Adeva *et al.* [LHCb Collaboration], “Roadmap for selected key measurements of LHCb”, v:0912.4179v2.
10. D. Karlen, “Using projections and correlations to approximate probability distributions”, *Comp. Phys.* **12** (1998) 380.
11. D. Martinez Santos, “Study of the very rare decay $B_s^0 \rightarrow \mu^+\mu^-$ in LHCb”, CERN-THESIS-2010-068.
12. K. Nakamura *et al.* [Particle Data Group], “Review of particle physics”, *J. Phys.* **G37** (2010) 075021.
13. D. Asner *et al.* [Heavy Flavour Averaging Group], “Averages of b -hadron, c -hadron, and τ -lepton properties”, arXiv:1010.1589. Updated values for f_d/f_s available at <http://www.slac.stanford.edu/xorg/hfag/osc/end.2009/> have been used for this document, as they include also pre-summer 2010 results which are not contained in¹².
14. R. Louvot, “Υ(5S) Results at BELLE”, arXiv:0905.4345v2.
15. E. Lopez Asamar *et al.*, “Measurement of trigger efficiencies and biases”, LHCb-PUB-2007-073.